Magnetic behavior of superconductor/ferromagnet superlattices

C. Monton, F. de la Cruz, and J. Guimpel
Centro Atómico Bariloche & Instituto Balseiro, Comisión Nacional de Energía Atómica & Universidad Nacional de Cuyo, (8400) San Carlos de Bariloche, Argentina

(Received 9 August 2006; revised manuscript received 15 November 2006; published 20 February 2007)

A study of the electromagnetic response of superconductor/ferromagnet Nb/Co superlattices is presented. The dc magnetization is measured as a function of Co layer thickness, applied field H_a, and temperature. For very thin Co layers, no ferromagnetism is detected and the observed response is essentially that of a collection of uncoupled Nb layers. When the Co layer is thick enough for ferromagnetism to be established, prior to the field-cooled magnetization measurements, the Co layers are magnetically saturated in the parallel or antiparallel directions to H_a. In this case, the magnetic response of the otherwise uncoupled Nb layers is found to depend on both H_a and the stray fields.

DOI: 10.1103/PhysRevB.75.064508 PACS number(s): 74.78.Fk, 75.70.Cn, 74.45.+c

I. INTRODUCTION

The superconducting/ferromagnetic (S/F) superlattice systems constitute an interesting test ground where the two materials interact at different levels. At the microscopic level, the proximity or exchange effects are present at the interfaces due to electronic wave functions extending from one material into the other.[1] At the macroscopic level, both materials show magnetic response, and the global magnetic state of the superlattice will be determined by their interaction.[2]

One of the most remarkable phenomena observed in this type of system is the unusual oscillatory dependence of the superconducting critical temperature T_{cs} on the ferromagnetic layer thickness. This behavior was predicted by Radovic *et al.*[3] in a microscopic proximity effect model, where π-junction coupling between adjacent superconducting layers was found. Jiang *et al.* experimentally verified this prediction in the Gd/Co system.[4]

Another interesting effect found in S/F superlattices[5] is the paramagnetic Meissner effect (PME). It was first observed in high-T_c materials, where it was considered as evidence for the existence of spontaneous supercurrents in the Meissner state caused by π junctions.[6] Later work showed that PME also appears in Nb discs,[7] and in twinned single crystals.[8] These results originated a new interpretation of the origin of the PME, based upon flux compression by Lorentz forces in thin samples.[9,10] Yet another explanation for the PME was proposed and verified, in which the effect is attributed to an experimental artifact due to combined effects of inhomogeneous sample cooling and magnetic field variation.[11] Recently, the PME was also reported in $YBa_2Cu_3O_7/La_{0.7}Ca_{0.3}MnO_3$ S/F superlattices.[5]

At a mesoscopic scale, for heterogeneous S/F systems with applied field perpendicular to the interface, it has been predicted that the stray fields at the domain walls could locally produce an enhancement of superconductivity.[12] In this scenario, it has been shown that there is an important contribution of stray fields.[2] It has also been shown in Nb/F bilayers, that superconductivity is enhanced when the magnetization of the ferromagnetic layer is very small.[13] In these experiments the superconducting magnetization was measured at constant applied field for different remnant moment of the ferromagnetic layers.

The possibility that a combination of these effects, i.e., π junctions, stray fields, and flux compression, is influencing the magnetic response of the S/F superlattices motivated us to investigate the superconducting magnetic response of Nb/Co superlattices by precise measurements of its Meissner flux expulsion for an applied magnetic field H_a parallel to the magnetic and superconducting layers. In this geometry the effects of stray fields are minimized due to the small demagnetization factor of each metallic layer and the sample as a whole. The flux expulsion in the superconducting layers is shown to be an extremely sensitive local magnetometer detecting the magnetic properties of the combined system. When the Co layers are less than 1 nm thick, ferromagnetism is quenched in the system and the magnetic response corresponds to a Meissner expulsion of a stack of independent superconducting layers. Despite the chosen geometry, the experiments make evident that the global superconducting behavior for thicker Co layers, where ferromagnetism is established, is determined not only by H_a but also by the small stray field penetrating into the superconducting layers.

II. EXPERIMENTAL DETAILS

The Nb/Co superlattices were grown on (001) Si substrates by standard dc magnetron sputtering. The vacuum system base pressure was 10^{-7} Torr and the sputtering gas was Ar at a total pressure of 10 mTorr. The deposition rate was 1.1 nm s^{-1} for Co and 0.7 nm s^{-1} for Nb. Under these conditions, Nb films show a superconducting transition temperature T_{cs} between 8 and 9 K, providing evidence for the high quality of the deposited film, given the known sensitivity of Nb's T_{cs} to contamination.[14] The layer thickness was controlled through deposition time. The substrate movement was computer controlled and the targets were automatically shut down during substrate movement, in order to avoid a nonlinear thickness vs deposition time relation due to the transit time of the substrate holder. Table I lists the characteristics of the studied superlattices. X-ray $\theta-2\theta$ diffraction scans were measured for superlattices with Co and Nb layer thicknesses $t_{Co}=t_{Nb}=2$ and 3 nm. The results show textured

TABLE I. Sample parameters. The table includes the Nb and Co nominal layer thicknesses t_{Nb} and t_{Co} the number of periods N, the superconducting critical temperature T_{cs}, the adjusted zero-temperature penetration depth $\lambda(0)$, the coercive field H_{coer}, the saturation magnetization M_S, and the Curie temperature T_{cm}.

t_{Nb} (nm)	t_{Co} (nm)	N	T_{cs} (K)	$\lambda(0)$ (nm)	H_{coer} (Oe)	M_S (emu cm^{-3})	T_{cm} (K)
44	7.5	19	5.9±0.1		26±2	1200±50	>300
44	5.0	20	6.7±0.3		120±4	950±10	>300
44	2.5	21	6.9±0.1		206±6	1250±50	>300
44	1.5	7	5.7±0.1		324±2	1100±50	155±5
44	1.0	7	7.4±0.1	44.7			
44	0.7	7	6.4±0.2	44.6			
44	0.5	7	6.6±0.1	47.0			

Nb(110)/Co(001) growth. Superlattice satellites are clearly observable around the main diffraction peaks indicating that individual layers are well defined. At low angles, total thickness size effect peaks are also observable. The period and total thickness extracted from the superlattice and size effect peak periodicity, respectively, agree with the nominal values within 10%.

In this work the superconducting magnetization of the superlattices was measured. The adequate experimental geometry for the measurement of the Meissner penetration depth in a film is with the applied field parallel to the surface. The flux expulsion in the Meissner state is determined by the magnetic penetration depth λ.[15] The magnetic field is continuous across the surface for this setup. The "perpendicular" geometry is appropriate for the measurement of the bulk upper critical field H_{c2}, since it is not modified by the sample thickness.[16] However, the demagnetizing factor is huge and its effects are dominant when the sample presents finite magnetization in the superconducting state.

The use of commercial superconducting quantum interference device (SQUID) magnetometer systems to measure the parallel magnetization M on thin film samples presents experimental difficulties. Sample to field alignment is difficult, if not impossible, to achieve. In the Meissner state, the signal generated by a long superconducting sample in the SQUID's coils is proportional to its cross-sectional area times the applied field. The cross-sectional area of a typical superlattice sample is of the order of a millimeter times 100 nm, i.e., 10^{-6} cm^2. If the sample is misaligned by an angle α, an applied field component proportional to $\sin\alpha$ will appear perpendicular to the sample surface. The sample Meissner magnetization in this direction will be proportional to this field value, times the sample area, approximately 1 mm^2, times the demagnetizating factor correction, proportional to sample radius divided by sample thickness, of the order 10^4. Of this magnetization value, a component, again, proportional to $\sin\alpha$ is captured by the detection coil. If this signal is to be smaller than the parallel one, then an upper limit of 0.006° for α is found. This is impossible to achieve in a magnetometer where the sample is displaced centimeters across the coil system. Even more, the estimated misalignment angle is an upper boundary, since flux penetration in λ from the surface was not considered, which will further reduce the parallel magnetization.

Also, given the huge demagnetizing factor correction for the perpendicular geometry, minor hysteresis loops in this direction will be traversed if the sample wobbles during movement, changing the misalignment angle and the perpendicular H component. This will clearly introduce artifacts in the data.[11]

The first inconvenience is greatly reduced for field-cooled (FC) measurements, where the sample is cooled down from above T_{cs} with H_a applied. In these experiments, perpendicular flux is trapped at T_{cs} as vortices and the perpendicular magnetization is greatly reduced. Thus the perpendicular signal becomes negligible when compared to the parallel one. The second inconvenientce can be avoided if the sample is not displaced during measurement. This implies that the measurement protocol often used in comercial SQUID magnetometers has to be changed. In our homemade SQUID magnetometer the SQUID's output signal is monitored continuously as the temperature T is swept without moving the sample. The signal is proportional to the *magnetization change* ΔM, and not to its absolute value.

Figure 1 shows a schematic cartoon of our homemade SQUID magnetometer.[17] A superconducting first-order gradiometer coil system made of Nb wire, is connected to a dc SQUID. The sample is located inside one of the coils. The gradiometer and sample are inside the bore of a superconducting magnet which, in persistent mode, applies a field H to the gradiometer region. The whole setup is built into a standard ^{4}He cryostat in such a way that the gradiometer,

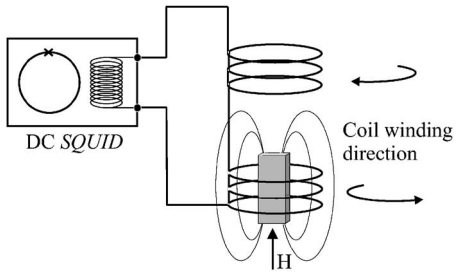

FIG. 1. Schematic drawing showing the experimental setup. The sample is located in one of the coils of a first-order gradiometer made of superconducting Nb wire. The gradiometer is hooked up to the input superconducting coil of a comercial dc SQUID. Magnetization changes on the sample generate magnetic flux changes in the coil, which induce superconducting currents in the gradiometer.

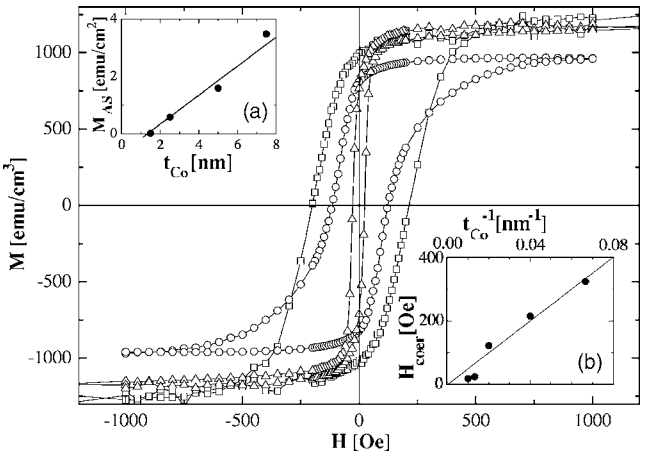

FIG. 2. Magnetization loops at 35 K for superlattices with different Co layer thicknesses. Open triangles, $t_{Co}=7.5$ nm; open circles, $t_{Co}=5$ nm; open squares, $t_{Co}=2.5$ nm. Inset (a), Saturation moment per unit area, M_{AS}, vs t_{Co}. The solid straight line is a guide to the eye. Inset (b) Coercive field H_{coer} vs. inverse of t_{Co}. The solid straight line is a guide to the eye. The magnetization data in the main panel were calculated with the Co volume excluding the dead layers at the interfaces.

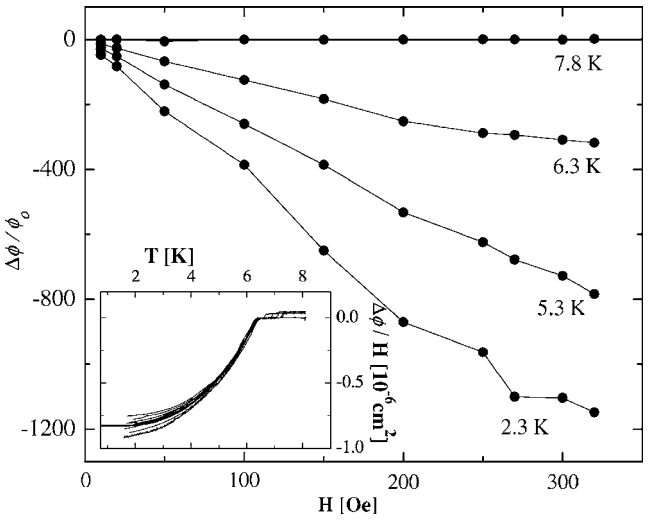

FIG. 3. Field-cooled magnetic flux expulsion H dependence at different T, for a superlattice with $t_{Co}=0.7$ nm. The linear H dependence is evidence of the sample being in the Meissner state for all the studied H range. The inset shows the field-cooled magnetic flux expulsion dependence in T, normalized by H. The solid line extending to lower T is the BCS clean limit dependence for $\lambda(0)=44$ nm and $2\Delta(0)/k_BT_{cs}=3.8$, where $\Delta(0)$ is the BCS zero-temperature gap value.

SQUID, and magnet are submerged in the constant-temperature ^{4}He bath. The sample is attached to a continuous evaporator[18] through a standard T control loop. When T is swept, the sample magnetization changes and fluxoid conservation in the gradiometer generates a current which is sensed by the SQUID. In this way, the magnetic flux changes, $\Delta\phi$, proportional to ΔM are measured. The flux sensitivity of the setup is $1\phi_0$, with ϕ_0 the fluxoid quantum, which for our typical sample geometry of 2 mm$\times$2 mm$\times$100 nm is roughly equivalent to 10^{-8} emu cm^{-3}. This system allows us to measure magnetic flux changes as a function of T in the range 1.4 to 10 K, for H up to 350 Oe.

III. RESULTS AND DISCUSSION

A. Magnetization in the normal state

For T larger than T_{cs}, the magnetic response of the superlattices is that of the Co layers. Figure 2 shows the parallel, i.e., easy axis for shape anisotropy, magnetization loops at 35 K for several superlattices with different Co layer thickness t_{Co} measured in a commercial SQUID magnetometer. In order to calculate the magnetization, the Co volume had to be corrected for the existence of a "dead layer" at the interfaces. Its existence is clearly seen in the inset (a) of the figure, where the saturation magnetic moment per unit area of the superlattice is shown as a function of t_{Co}. The linear dependence which extrapolates to zero moment at a finite t_{Co} of around 1 nm, indicates a dead layer thickness of around 0.5 nm at each interface.[19]

After subtracting the dead Co volume represented by this thickness times the number of Co/Nb interfaces, the data in Fig. 2 are obtained. Two features are distinct. First, the saturation magnetization M_s of around 1200 emu cm^{-3} is near that of bulk Co, 1400 emu cm^{-3}, independent of t_{Co}. Second, the inset (b) shows that H_{coer} increases with decreasing t_{Co}. This behavior indicates that the Co films are in the multidomain regime with domain reversal accomplished through Bloch wall motion.[22]

The existence of the dead layer at the interfaces implies that for $t_{Co}<1$ nm ferromagnetism is not established and the Co layers will probably act as pair breaking regions, depressing or suppressing the superconducting properties at the interfaces. For $t_{Co}>1$ nm ferromagnetism is present and stray field effects due to Co layer remanent magnetization may also be observed. The next two subsections will present our results for these two cases.

B. Thin Co layers ($t_{Co}<1$ nm)

Figure 3 shows the parallel FC flux expulsion dependence on H_a and T for the $t_{Co}=0.7$ nm superlattice. The flux expulsion is defined as $\Delta\phi=\phi_s-\phi_n$, where ϕ_s and ϕ_n are the magnetic flux through the sample in the superconducting and normal states, respectively. The main panel shows $\Delta\phi$ vs H_a at different temperatures, and the inset shows the ratio $\Delta\phi/H_a$ as a function of T for different applied fields. Similar behavior is observed for all superlattices with $t_{Co}<1$ nm. The linear H_a dependence observed in the data is the behavior expected for a superconductor in the Meissner state. The flux expulsion for an infinite rectangular slab parallel to the field, with thickness t, width $W\gg t$, and penetration depth $\lambda(T)$, is given by

$$\frac{\Delta\phi}{H_a}=W\left(2\lambda(T)\tanh\frac{t}{2\lambda(T)}-t\right) \quad (1)$$

which is a function independent of field. The small nonscaling of the data at low temperatures may be due to some

remanent ferromagnetism of the thin Co layers, nonobservable with a commercial SQUID due to their smaller sensitivity.

The temperature dependence of the data indicates that the penetration depth is of the order of the film thickness. However, in order to assign a numerical value to λ two posible pictures can be applied. In one, the superconducting Nb films are decoupled by the Co layers.[19] In this case, the film thickness to be used in Eq. (1) is t_{Nb} and the calculated $\Delta\phi$ has to be multiplied by the number of Nb layers in the superlattice. The zero-temperature $\lambda(0)$ values were adjusted by fitting the data with the BCS temperature dependence for λ. The results are included in Table I. These values explain why there is no evidence of superconducting vortices in the measured H_a range. A $\lambda(0)$ of around 40 nm implies a value of the first critical field $H_{c1}(0)$ of around 1000 Oe for bulk Nb. Moreover, since the film thickness is of the order of $\lambda(0)$, size effects are important.[20] The size-effect-corrected first critical field is given by

$$\tilde{H}_{c1}(T) = \frac{H_{c1}(T)}{1 - \left[\cosh\left(\frac{t}{2\lambda(T)}\right)\right]^{-1}} \times \left[1 + \frac{2}{\ln\kappa}\sum_{j=1}^{\infty}(-1)^j K_0\left(\frac{jt}{\lambda(T)}\right)\right] \quad (2)$$

where K_0 is the second-order modified Bessel function. This field is almost T independent and has a value of around 1 T. It is important to remark that in a FC experiment the mixed state is traversed between H_{c2} and H_{c1} on cooling down and vortices could remain trapped. However, the huge value of $\tilde{H}_{c1}$, and the fact that it is reached almost immediately after entering the superconducting state, makes the trapped vortices highly thermodynamically unstable, and they are expelled leaving the sample in the ground Meissner state.

The other posible picture is that of coupled Nb layers, in which case the thickness to be used in Eq. (1) is the total superlattice thickness. In this case, values of λ of the order of several hundreds of nanometers are obtained, which imply values of $H_{c1}(0)$ of around 10 Oe and of $\tilde{H}_{c1}(0)$ of around 100 Oe, clearly incompatible with the lack of vortices up to 350 Oe. Our conclusion is, then, that the very thin Co layers, either continuous or granular in nature, are acting as pair-breaking layers, suppressing superconductivity and completely decoupling the Nb layers.

An interesting point is that the adjusted λ values are similar to that of pure Nb, which is 39 nm. This indicates that the order parameter in the Nb layers is not depressed, in spite of the decoupling induced by the Co layers.

Figure 3 includes the clean limit BCS prediction, using the nominal t_{Nb}, $\lambda(0)=44$ nm, and the Nb value for the superconducting gap, $2\Delta(0)/k_B T_{cs}=3.8$. This prediction agrees well with the data, within the experimental uncertainty.

C. Thick Co layers ($t_{\mathrm{Co}}>1$ nm)

When the Co layers present ferromagnetic behavior, their magnetic state has to be taken into consideration when preparing the initial state for superconductivity FC measurements. Two different initial states were prepared. In the first one, +FC, the Co layers were saturated in the parallel (positive) direction with respect to H_a, with 350 Oe before applying a positive H_a for measuring the superconducting flux variation. In the second, −FC, the Co layers were saturated in the antiparallel (negative) direction before applying a positive H_a. In this way, the +FC and −FC magnetization measurements were performed with the Co layers magnetized in the corresponding branches of the hysteresis loop (see Fig. 2). The T dependence of the Co layer's magnetization will not be observed in the experiments, since they are performed at temperatures much lower than their Curie temperature T_{cm}.

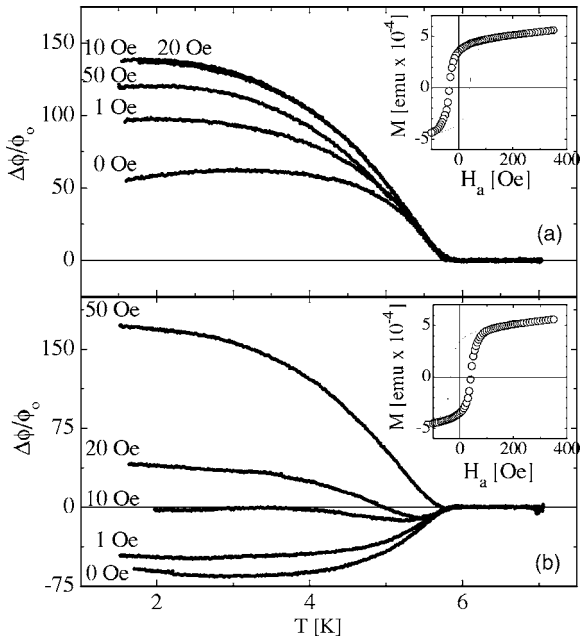

FIG. 4. Field-cooled magnetic flux expulsion T dependence for a superlattice with $t_{\mathrm{Co}}=7.5$ nm. (a) +FC, and (b) −FC experiments. The applied fields are labeled in the figure. The coercive field for this sample is $H_{coer}=26$Oe at 35 K. For zero external field the signal is finite, signaling the Nb layer response to the Co layer stray field. Insets show with open circles the magnetic state of the Co layers for each kind of experiment.

Figures 4(a) and 4(b) show the temperature dependence of the flux expulsion $\Delta\phi$ induced in the superconducting state of a superlattice with $t_{\mathrm{Co}}=7.5$ nm for the +FC and −FC initial states, respectively. Similar response was found for all superlattices with $t_{\mathrm{Co}}>1$ nm. It is obvious that the flux expulsion behavior in both configurations is not that expected for a homogeneous superconducting state. In Fig. 4(a) we see that, for +FC, $\Delta\phi>0$ for all H_a, instead of the negative values expected for flux expulsion of a homogeneous superconductor. Contrasting this behavior, the −FC data in Fig. 4(b) show a diamagnetic response for low fields that becomes paramagnetic for high enough fields. This, plus the nonlinear relation between the H_a and $\Delta\phi$, and the finite reversed $\Delta\phi$ observed for $H_a=0$ for both configurations, hint at the possibility of stray field effects induced by the magnetic layers influencing the magnetic response of the super-

conducting state. In fact, if the Co layers are magnetized in the positive (negative) direction a negative (positive) stray field is expected to be present on the Nb layers above T_{cs}. The results in Fig. 4 make evident that, under the experimental conditions described in this work, there is no superconducting phase coherence across the superlattice. Also, the results for $H_a=0$ strongly suggest that, despite the extremely small demagnetization factor of the magnetic and superconducting layers, the stray fields are responsible for the field expulsion of independent (decoupled) superconducting layers.

Another interesting qualitative result is shown in Fig. 4(b) for the −FC flux expulsion at H_a close to the coercive field, where the change in sign of $\Delta\phi$ resembles the paramagnetic Meissner effect previously reported in superconducting and superconducting/ferromagnet systems.[5,6,21] In Ref. 5 it is shown that the PME is related to the granular character of the F layer. This is not the case for our samples, since we observe this effect for all t_{Co}, including those with a hysteresis loop shown in fig. 2, clearly nongranular.

From the previous discussion of the flux expulsion results it becomes apparent that superconductivity in the different layers is uncorrelated. Consequently, we can use the magnetic flux expulsion as described by expression (1) as a local magnetometer detecting the effective magnetic field H_{eff} in the Nb layers. The nonmonotonic T dependence of $\Delta\phi$ for H_a close to the coercive field in the −FC configuration makes evident that H_{eff} is a temperature-dependent field. This indicates that the flux expulsion from the superconducting layers modifies the magnetic state of the Co layers. In order to avoid this inconvenience we use the slope of the flux expulsion at T_{cs}, $(\partial\Delta\phi/\partial T)|_{T_c}$, as a detector of H_{eff} at a well-defined magnetic state of the Co layers. At T_{cs}, superconductivity is just nucleated and the small magnetization of the Nb layers does not affect the magnetic state of the F layers. Thus, H_{eff} can be determined from the BCS fitting of the flux expulsion of uncorrelated superconducting layers, where it is the only fitting parameter. As an example of the fitting procedure described above, we show in the inset of Fig. 5 the temperature dependence of the flux expulsion for $H_a=0$ (−FC configuration) together with the best BCS fitting of the flux expulsion close to T_{cs}. In the fitting $\lambda(0)=44$ nm is the same used in the inset of Fig. 3. The result shows $H_{eff}=23$ Oe for this superlattice. This value of the stray field corresponds to the Co layers being at the remanent magnetization value for the lower branch of the magnetization loop (see detail in the inset of the lower panel in Fig. 4).

It is clear from the inset in Fig. 5 that, contrary to what is shown for the very thin magnetic layers, the expected theoretical flux expulsion fits the data only close to T_{cs}. For lower temperatures the disagreement between the theoretical expectation and experiments is evident. This indicates that the stray field changes with temperature as a result of the flux expulsion from the Nb layers. This drives the stray field lines to partially close outside the superlattice, thus decreasing H_{eff} on the superconducting layers. At present we can only describe qualitatively this unusual magnetic behavior in superlattices.

Figure 5 shows H_{eff} as a function of H_a for both +FC and −FC cases, as obtained from the fitting of the flux expulsion.

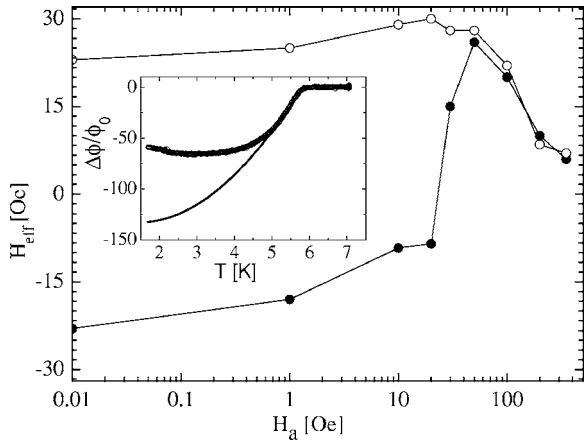

FIG. 5. Effective field as a function of H_a for $t_{Co}=7.5$ nm superlattice. Open circles, +FC initial state; solid circles, -FC initial state. See text for −FC and −FC initial state descriptions. Inset shows the −FC flux expulsion for $H_a=0$ and the best fit to the data near T_{cs} with the clean limit BCS dependence for $\lambda(0)=44$ nm, $2\Delta(0)/k_BT_{cs}=3.8$, and an effective field of 23 Oe.

In the +FC case the weak H_a dependence at low applied fields is mainly due to the weak expected change of the stray field, proportional to the Co magnetization, as inferred from the upper branch of the Co hysteresis loop [see inset in Fig. 4(a)]. With further increase of H_a the applied field is no longer negligible. For $H_a>200$ Oe, the competition between the positive H_a and the negative stray field originates a reduction of H_{eff} and the positive flux expulsion diminishes. The −FC data show a different dependence. At the low H_a region, the behavior of H_{eff} is similar to that in the +FC configuration although reversed in sign and with a somewhat stronger H_a dependence. In this case, the magnetic state of the Co layers is described by the lower branch of the magnetization loop [see inset in Fig. 4(b)]. At intermediate fields, when H_a exceeds the coercive field, the negatively magnetized Co layers reverse, reversing also the stray field, which becomes opposite to H_a, and the flux expulsion changes sign. For higher H_a the lower branch of the magnetization loop approaches that of the upper one, and the effective field tends to that of the +FC configuration.

One important difference between the +FC and −FC responses should be taken into account. In the first case the positively magnetized Co layers do not show an appreciable H_a dependence since they are already magnetized in the applied field direction, while in the −FC configuration the increase of H_a implies the reversal of the Co magnetization, through a magnetically disordered distribution of domains. This difference should be taken into account by any model trying to describe H_{eff} for temperatures well below T_{cs}.

IV. CONCLUSIONS

Summarizing, the magnetic response of superconducting/ferromagnetic Nb/Co superlattices has been studied. For very thin magnetic layers ferromagnetism is not detected. For thicker layers ferromagnetism is established in the Co layers. The experimental results demonstrate that in both

cases the superlattice behaves as a collection of noncoupled superconducting layers. The temperature dependence of the superconducting flux expulsion for superlattices with thin Co layers is well fitted by the standard BCS theoretical expressions with the values of bulk Nb for the T-dependent penetration depth. It is important to remark that the Meissner flux expulsion (lack of remanent pinned vortices) detected in FC measurements is due to the high value of $H_{c1}(T)$ associated with the superconducting size effect in the Nb layers. For the superlattices with thick Co layers, the overall temperature-dependent magnetic response is quantitatively understood within a picture where the stray fields induced in the Nb layers are superimposed on the applied field. This effect becomes so important as to invert the field direction with respect to the applied field, giving rise to a signal resembling that of the paramagnetic Meissner effect.[5,6,21]

Two explanations have been offered for the paramagnetic Meissner effect based on different hypotheses. From the microscopic point of view, the Wohlleben effect[6] relies on permanent supercurrents flowing in π junctions due to nonconventional superconducting pairing. It has been predicted that in S/F superlattices there is also the possibility of the existence of π junctions,[3] dependent on the ferromagnet thickness, a prediction that has been experimentally confirmed through the induced oscillations in T_{cs}.[4] In our experiments, we observe a superconducting PME-like signal for all t_{Co} thicker than the dead layer, making unlikely this microscopic explanation. The other possible explanation based on macroscopic flux trapping should be ruled out,[11] since in these experiments the sample is not moved and field variations cannot be invoked.

The experimental data show that in the range of magnetic fields and temperature investigated there is no superconductivity induced across the magnetic layers. The decoupling between superconducting layers is possibly due to the pair-breaking mechanism induced by the magnetic dead layer at the interfaces. The magnetic Meissner response of the superconducting layers has been shown to be an excellent local magnetometer to study the magnetic behavior of superlattices. The analysis of the flux expulsion close to $T_{cs}(H)$ made evident unexpected results for superlattices with ferromagnetic Co layers. In this case, the magnetic field in the Nb layers at the superconducting transition is shown to be the linear sum of the stray field induced by the Co layers and the fraction of the applied field penetrating into the Nb layers above T_{cs}. In this case the results show that the external applied field is not the variable controlling the experiment. On the other hand, at lower temperatures the magnetic response shows that the Meissner flux expulsion of the Nb modifies the magnetic state of the Co layers, making evident the interplay between magnetism and superconductivity in the global response of superlattices. In this configuration the experimental results show that conservation of magnetic flux through the superlattice is not the adequate control variable. These important effects make clear the relevance of nonideal geometrical configuration effects in most of the experiments with magnetic hybrids. Due to geometrical effects the often assumed external variables that control the experiments as external magnetic field or flux conservation is incorrect.

ACKNOWLEDGMENTS

This work was partially supported by ANPCyT Grants No. PICT2003-03-13511 and No. PICT2003-03-13297 and Fundación Antorchas.

[1] A. I. Buzdin, Rev. Mod. Phys. **77**, 935 (2005).
[2] Z. Yang, M. Lange, A. Volodin, R. Szymczak, and V. V. Moschalkov, Nat. Mater. **3**, 793 (2004).
[3] Z. Radović, M. Ledvij, L. Dobrosavljević-Grujić, A. I. Buzdin, and J. R. Clem, Phys. Rev. B **44**, 759 (1991).
[4] J. S. Jiang, D. Davidović, D. H. Reich, and C. L. Chien, Phys. Rev. Lett. **74**, 314 (1995).
[5] M. A. López de la Torre, V. Peña, Z. Sefrioui, D. Arias, C. Leon, J. Santamaria, and J. L. Martinez, Phys. Rev. B **73**, 052503 (2006).
[6] W. Braunisch, N. Knauf, V. Kataev, S. Neuhausen, A. Grütz, A. Kock, B. Roden, D. Khomskii, and D. Wohlleben, Phys. Rev. Lett. **68**, 1908 (1992).
[7] D. J. Thompson, M. S. M. Minhaj, L. E. Wenger, and J. T. Chen, Phys. Rev. Lett. **75**, 529 (1995).
[8] S. Riedling, G. Bräuchle, R. Lucht, K. Röhberg, H. v. Löhneysen, H. Claus, A. Erb, and G. Müller-Vogt, Phys. Rev. B **49**, 13283 (1994).
[9] A. E. Koshelev and A. I. Larkin, Phys. Rev. B **52**, 13559 (1995).
[10] V. V. Moshchalkov, X. G. Qiu, and V. Bruyndoncx, Phys. Rev. B **55**, 11793 (1997).
[11] F. J. Blunt, A. R. Perry, A. M. Campbell, and R. S. Liu, Physica C **175**, 539 (1991).
[12] A. Yu. Aladyshkin, A. I. Buzdin, A. A. Fraerman, A. S. Mel'nikov, D. A. Ryzhov, and A. V. Sokolov, Phys. Rev. B **68**, 184508 (2003).
[13] D. Stamopoulos and M. Pissas, Phys. Rev. B **73**, 132502 (2006).
[14] J. E. Crow, M. Strongin, R. S. Thomson, and O. F. Kammerer, Phys. Lett. **30A**, 161 (1969).
[15] J. Guimpel, F. de la Cruz, J. Murduck, and I. K. Schuller, Phys. Rev. B **35**, 3655 (1987).
[16] M. Tinkham, *Introduction to Superconductivity*, 2nd ed., (McGraw-Hill, New York, 1996) p. 136.
[17] R. Arce, F. de la Cruz, and P. Esquinazi, Solid State Commun. **38**, 1253 (1981).
[18] L. E. DeLong, O. G. Symko, and J. C. Wheatley, Rev. Sci. Instrum. **42**, 147 (1971).
[19] P. Koorevaar, Y. Suzuki, R. Coehoorn, and J. Aarts, Phys. Rev. B **49**, 441 (1994).
[20] J. Guimpel, L. Civale, F. de la Cruz, J. M. Murduck, and I. K. Schuller, Phys. Rev. B **38**, 2342 (1988).
[21] T. M. Chuang, S. F. Lee, S. Y. Huang, Y. D. Yao, W. C. Cheng, and G. R. Huang, J. Magn. Magn. Mater. **239**, 301 (2002).
[22] B. D. Cullity, *Introduction to Magnetic Materials* (Addison-Wesley, Reading, MA, 1972) p. 385.